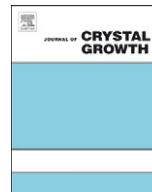




ELSEVIER

Contents lists available at ScienceDirect

Journal of Crystal Growth

journal homepage: www.elsevier.com/locate/jcrysgr

MBE growth of high conductivity single and multiple AlN/GaN heterojunctions

Yu Cao ^{*}, Kejia Wang, Guowang Li, Tom Kosel, Huili Xing, Debdeep Jena

Department of Electrical Engineering, University of Notre Dame, IN 46556, USA

ARTICLE INFO

Available online 21 December 2010

Keywords:

A1. AlN

A1. 2DEG

A1. TEM

A1. XRD

A3. MBE

B3. Heterojunction

ABSTRACT

Record-low sheet-resistance of $\sim 128 \Omega/\text{sq}$ have been obtained in two-dimensional electron gases at ultrathin single AlN/GaN heterojunctions by optimizing the metal fluxes used in molecular beam epitaxy growth. Multiple 2DEGs have been found in AlN/GaN superlattices, with the net electron density measured $> 1 \times 10^{14} \text{ cm}^{-2}$ at room temperature. This very high electron density also leads to a further lowering of sheet resistance to values far below what is achievable in single nitride heterojunctions. These low resistance channels are induced entirely by polarization in nominally undoped heterostructures, and are attractive for various device applications such as high speed transistors and intersubband detectors.

Published by Elsevier B.V.

1. Introduction

It has been shown that at single AlN/GaN heterojunctions, two-dimensional electron gases (2DEGs) with sheet densities up to $\sim 6 \times 10^{13} / \text{cm}^2$ are achievable, with the sheet resistance as low as $150 \Omega/\text{sq}$ [1,2]. High electron mobility transistors (HEMTs) fabricated with such structures have shown high current densities more than 2.3 A/mm and transconductances up to 480 mS/mm [3]. Buffer leakage problems in such HEMTs have also been solved using ultrathin AlN back-barriers [4]. These results have shown that AlN/GaN heterojunctions are promising to push the performance of GaN HEMTs into a new level which the traditional AlGaIn/GaN HEMTs are not able to reach.

When grown lattice-matched to GaN, the AlN barrier has to be thinner than 5 nm to avoid strain relaxation [5]. An improved AlN/GaN interface has been proven to be important to achieve high 2DEG mobility and hence lower the sheet resistance [1]. These requirements sensitively depend on the MBE growth conditions. We find that the metal fluxes used in MBE growths showed important effects on the 2DEG transport properties in both single and multiple AlN/GaN heterojunctions. By optimizing the metal fluxes, a record-low sheet resistance of $\sim 128 \Omega/\text{sq}$ has been achieved in single as-grown AlN/GaN heterojunctions. Using the optimal fluxes found for single AlN/GaN heterojunctions, high-mobility 2DEGs are found in AlN/GaN multiple quantum wells (MQWs). The details of these findings are discussed in this paper.

2. Single AlN/GaN heterojunctions

The AlN/GaN heterojunctions studied here were grown by MBE in a Veeco Gen 930 system on Fe-doped semi-insulating $1 \times 1 \text{ cm}^2$ GaN templates prepared by metalorganic chemical vapor deposition (MOCVD) on sapphire. Active N_2 was supplied through a Veeco RF plasma source with the plasma power of 275 W, which yielded a growth rate of $\sim 210 \text{ nm/h}$. The N_2 pressure at the substrate position was kept constant at $\sim 2 \times 10^{-5} \text{ Torr}$ which provided the nitrogen flux $F_{\text{N}} < 1.5 \times 10^{-7} \text{ Torr}$. The Ga and Al fluxes were kept at $F_{\text{Ga}} \sim 1.55 \times 10^{-7} \text{ Torr}$ and $F_{\text{Al}} \sim 1.50 \times 10^{-7} \text{ Torr}$ separately. These metal fluxes guaranteed the growths were performed in the metal-rich regime.

Although a thin AlN back barrier grown in N-rich regime can effectively remove the parasitic channel at the regrowth interface [4], to make a consistent study of metal flux effect on transport properties, the same growth procedure was performed as those in previous report [1,5]. Ga was deposited on the substrate for 10 s ($\sim 2 \text{ MLs}$) at a substrate thermocouple temperature $T_c = 600 \text{ }^\circ\text{C}$. Then the nitrogen shutter was opened, and T_c was linearly ramped up to $660 \text{ }^\circ\text{C}$ in 3 min. The following GaN buffer layer and AlN barrier were grown at $T_c = 660 \text{ }^\circ\text{C}$. Ga was used as surfactant during AlN barrier growth. The substrate was rotated at 30 rpm to enhance the uniformity of the grown epilayers. The $1 \times 1 \text{ cm}^2$ samples were mounted on 3-in double-side lapped silicon wafers with indium. The thickness of the lapped silicon wafers varies between 500 and 700 μm , which is not uniform. Since the silicon wafer locates between the thermocouple and the GaN template during growth, the real growth temperature changes with the silicon wafer thickness. To make the results more conclusive, optimization has to be done based on statistical results. Four samples were grown at each flux setting. In this way, the effect of silicon wafer thickness and mounting with indium can be partially excluded.

^{*} Corresponding author. Tel.: +1 574 631 1290.

E-mail addresses: ycao1@nd.edu, cy.yuca@gmail.com (Y. Cao).

To investigate the effect of the metal fluxes on the 2DEG transport properties in single AlN/GaN heterojunctions, the Al and Ga fluxes were varied alternately. One metal flux was changed over a range of $\sim 2 \times 10^{-8}$ Torr with the other metal flux fixed, and this iteration swapped. Iterations continued until the saddle points for lowest sheet resistance for Ga and Al fluxes were found. After each growth, Hall-effect measurements were performed at room temperature and 77 K. Fixing one metal flux at the value where the lowest sheet resistance was achieved, the other metal flux was changed in the given range again, followed by the Hall-effect measurements. After several iterations, we were able to find the saddle point of the sheet resistance with the optimized Al and Ga

fluxes of $F_{Al} \sim 1.50 \times 10^{-7}$ Torr and $F_{Ga} \sim 1.61 \times 10^{-7}$ Torr. Fig. 1(a) shows the RT sheet resistance dependence on the Ga flux at a fixed Al flux, indicating an optimized Ga flux $F_{Ga} \sim 1.61 \times 10^{-7}$ Torr. Fig. 1(b) shows that the optimized Al flux to be $F_{Al} \sim 1.50 \times 10^{-7}$ Torr. This improvement in growth directly lead to improved transport properties shown in Fig. 2(a) and (b), compared with our previous report [1,5]. The highest mobility achieved with optimized fluxes is ~ 1900 cm²/Vs at RT and ~ 8000 cm²/Vs at 77 K for an AlN barrier thickness of ~ 2.3 nm, with a 2DEG density of 1.1×10^{13} cm⁻² at RT. As Fig. 3 indicates, the lowest RT sheet resistance achieved is 128.6 Ω/\square , with a 3.5 nm AlN cap. This is the lowest sheet resistance reported to date in 2DEGs in as-grown III–V nitride heterojunctions, and is highly

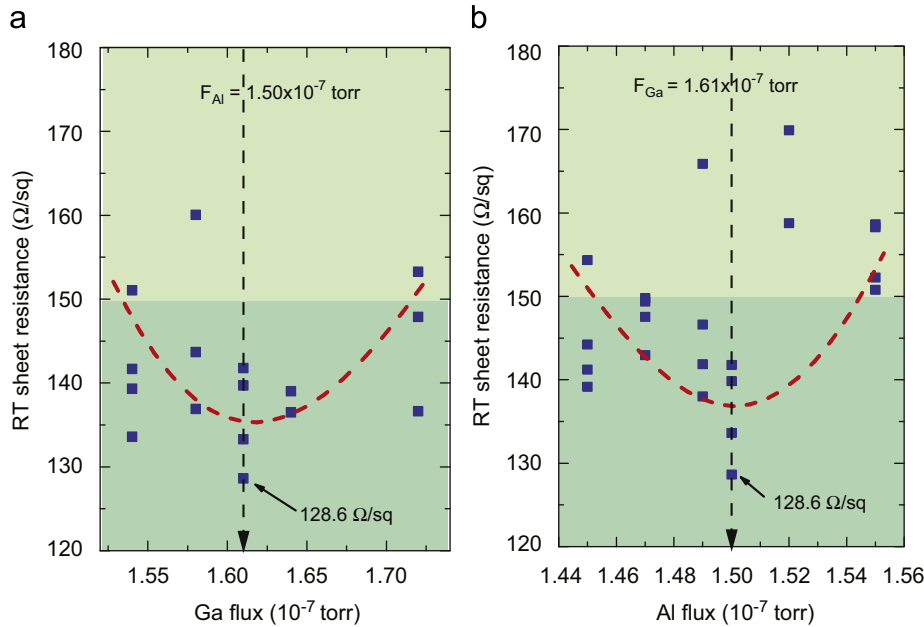


Fig. 1. The sheet resistance measured at RT with (a) different Ga flux and (a) different Al flux.

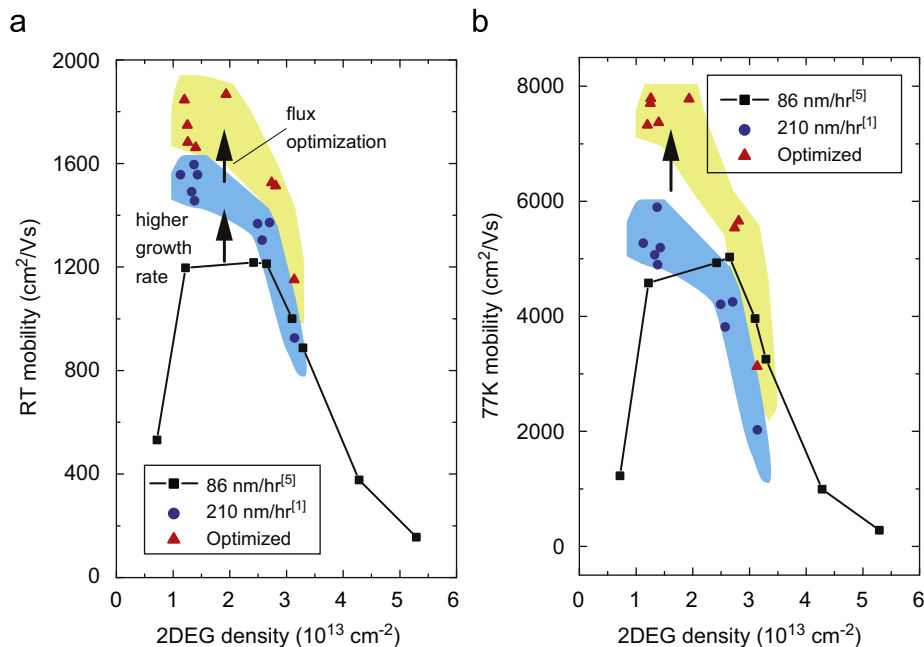


Fig. 2. With flux optimization, the enhancement in the (a) RT and (b) 77 K mobility is shown compared to previous reported values. This growth improvement lead to the record-low sheet resistance in all reported as-grown nitride HEMTs, which is shown in (c) where the sheet resistance is plotted against the 2DEG density.

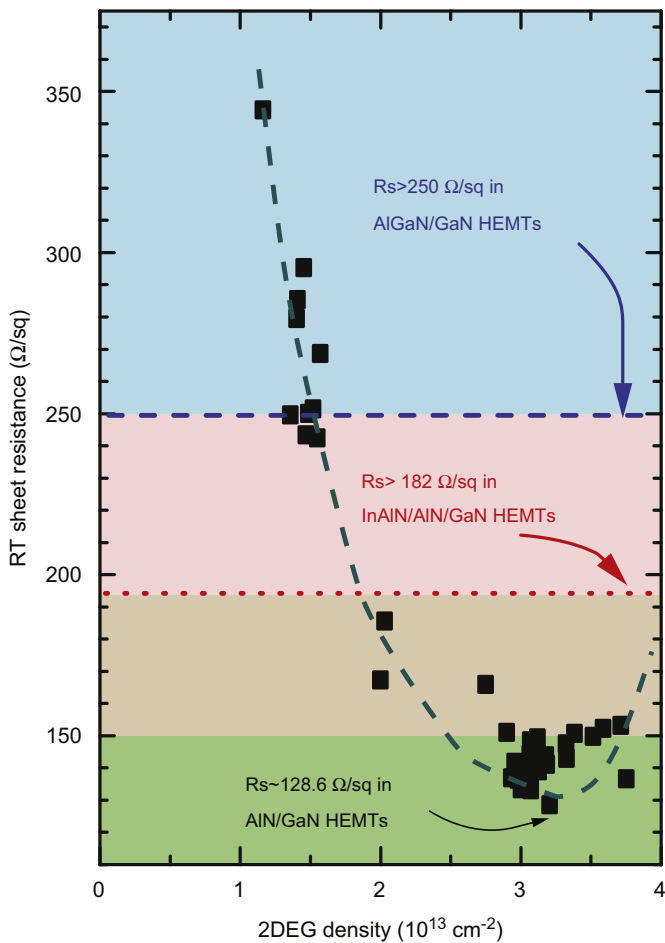


Fig. 3. With flux optimization, record-low sheet resistance is achieved in as-grown AlN/GaN HEMT structures.

attractive for the reduction of parasitic access resistances in high-speed HEMT design. Hall-effect measurements made on this sample showed a 2DEG mobility of $1513 \text{ cm}^2/\text{Vs}$ at RT and $5655 \text{ cm}^2/\text{Vs}$ at 77 K, with the 2DEG density of $3.21 \times 10^{13} \text{ cm}^{-2}$ at RT and $2.81 \times 10^{13} \text{ cm}^{-2}$ at 77 K, respectively. To our knowledge, the lowest sheet resistance reported in AlGaIn/GaN heterostructures is $\sim 250 \text{ } \Omega/\square$ [6] and $182 \text{ } \Omega/\square$ in InAlN/AlN/GaN system [7]. A lower sheet resistance of $172 \text{ } \Omega/\square$ was achieved with AlN/GaN superlattices (SLs) [8]. In the GaN/AlN/GaN heterostructures, the sheet resistance reported is as low as $\sim 140 \text{ } \Omega/\square$ [2].

As discussed in our previous report [5], the RT mobility of the 2DEGs in these samples is determined by the combination of polar optical phonon (POP) scattering, acoustic phonon (AP) scattering, and interface roughness (IR) scattering. At RT, though POP scattering is the dominant mechanism, IR scattering and AP scattering have a measurable effect. At 77 K, the POP and AP scattering are negligible, and the effect of IR scattering can be clearly identified. By optimizing the metal fluxes, the AlN/GaN heterointerface was improved and electrons suffer less IR scattering, leading to an enhancement of the 2DEG transport properties.

3. Multiple AlN/GaN heterojunctions

In $[(\text{AlN})_a](\text{GaIn})_b)_N$ multiple quantum wells (MQWs), where a and b refer to the thickness of AlN and GaN, respectively, and N is the number of periods, more than one 2DEG can exist between AlN/GaN heterojunctions [10]. Although ohmic contacts and gate

modulation might be a concern for using such multiple heterojunctions in traditional HEMT layout, it is attractive for nanowire-based electronic devices with wrapped gates to achieve high-speed performance and good gate modulation. Intersubband detector is also one attractive application.

An $[(\text{AlN})_a](\text{GaIn})_b)_7$ MQW sample was grown with $N = 7$ periods with $a = 2.6 \text{ nm}$ and $b = 55.2 \text{ nm}$, and used for transmission electron microscopy (TEM) study. The cross-section TEM sample was prepared by mechanical wedge polishing at 2° , followed by ion-milling at 2 keV. TEM imaging was performed on a JEOL 2010 system with 200 kV accelerating voltage. Fig. 4(a) shows sharp AlN/GaN heterointerfaces. As Sang et al. pointed out, multiple interfaces in MQWs are efficient in terminating threading dislocations (TDs) [11]. Fig. 4(b) shows that a TD is terminated at the first AlN/GaN heterointerface.

The net in-plane sheet carrier density can be much higher in a MQW structure than that achievable from single heterojunctions if multiple 2DEGs are formed. To test this, a series of $[(\text{AlN})_a](\text{GaIn})_b)_N$ MQW samples were grown by MBE with N varying from 1 to 6. The structure in each period has $a = 2.6 \text{ nm}$ AlN and $b = 30 \text{ nm}$ GaN. The carrier concentrations were measured by Hall-effect measurements. Except the discrepancy with 5 periods, the net measured sheet carrier concentration increases with N , as shown in Fig. 5(b). The energy band diagram simulated by 1D Poisson [9] is shown in the insert of Fig. 5, indicating that conducting channels exist in each period. In Fig. 5(b), The measured 2DEG mobility decreases with increasing the period number, in agreement with a previous report [10]. The degradation of 2DEG mobility can be due to excessive Ga metal. The Ga shutter was open during the growth of the AlN layer. Ga atoms only served as surfactants and did not enter alloy.

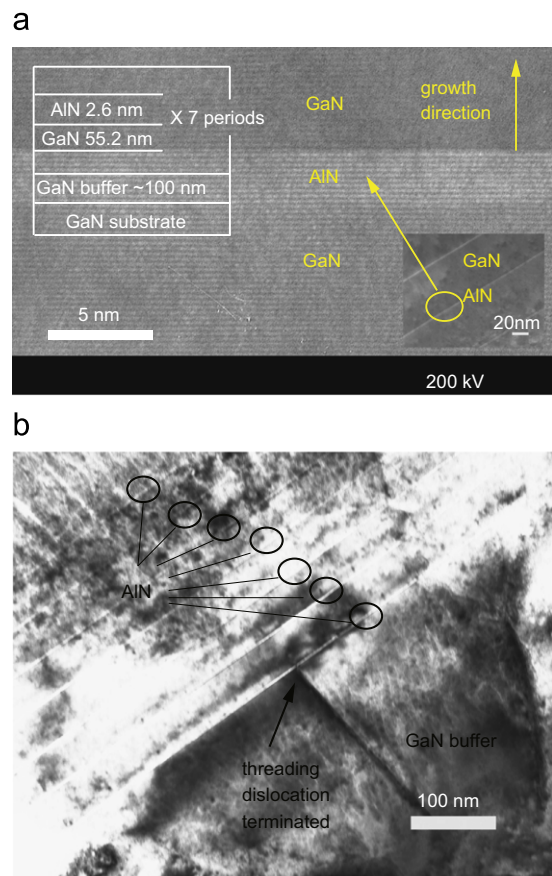


Fig. 4. In AlN/GaN SLs, (a) the TEM lattice image showed sharp interfaces between AlN/GaN. (b) The bright field image shows one threading dislocation is terminated at the first AlN/GaN heterointerface.

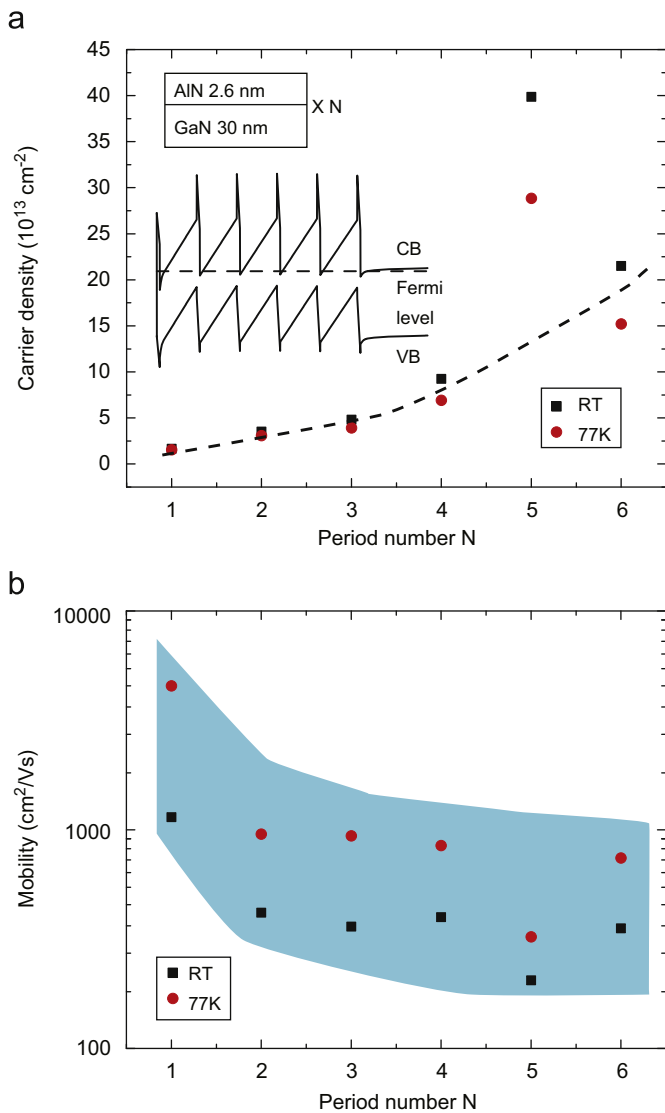


Fig. 5. Multiple 2DEGs were found in the AlN/GaN SLs with (a) the total 2DEG density and (b) 2DEGs mobility at RT and 77 K plotted against the period number N . The insert in (a) shows the band diagram of a 6-period AlN/GaN MQWs.

Therefore, Ga metal will keep accumulating on the sample surface after each period, leading to the degradation of 2DEG transport properties of the 2DEGs in the QWs nearer to the surface, as indicated by the results in Fig. 1(a).

To reduce the Ga accumulation on the surface, a lower Ga flux is desired. A 9 period AlN/GaN MQWs was grown with a lower RF power of 150 W, at a growth rate $\sim 156 \text{ nm/h}$. The Ga and Al fluxes were lowered to $F_{\text{Ga}} \sim 1.02 \times 10^{-7} \text{ Torr}$ and $F_{\text{Al}} \sim 4.16 \times 10^{-8} \text{ Torr}$. To prevent Ga accumulation, a higher substrate temperature is also desired to reduce the Ga accumulation during the growth of AlN layers. The sample was mounted In-free. The substrate heater was directly behind the sample. Tungsten was deposited on the back of the sample to enhance the thermal uniformity. In this way, higher substrate temperature can be achieved without worrying the sample to slide off the silicon wafer. The thermocouple temperature used for this growth was $T_{\text{TC}} \sim 800 \text{ }^\circ\text{C}$, providing the same substrate temperature as $T_{\text{TC}} \sim 680 \text{ }^\circ\text{C}$ under the indium-mounted condition.

The signature of multiple AlN/GaN heterojunctions can be directly found by X-ray diffraction (XRD) measurement. Fig. 6(a) shows the XRD spectra for a 9 period AlN/GaN MQW structure. The well-defined and

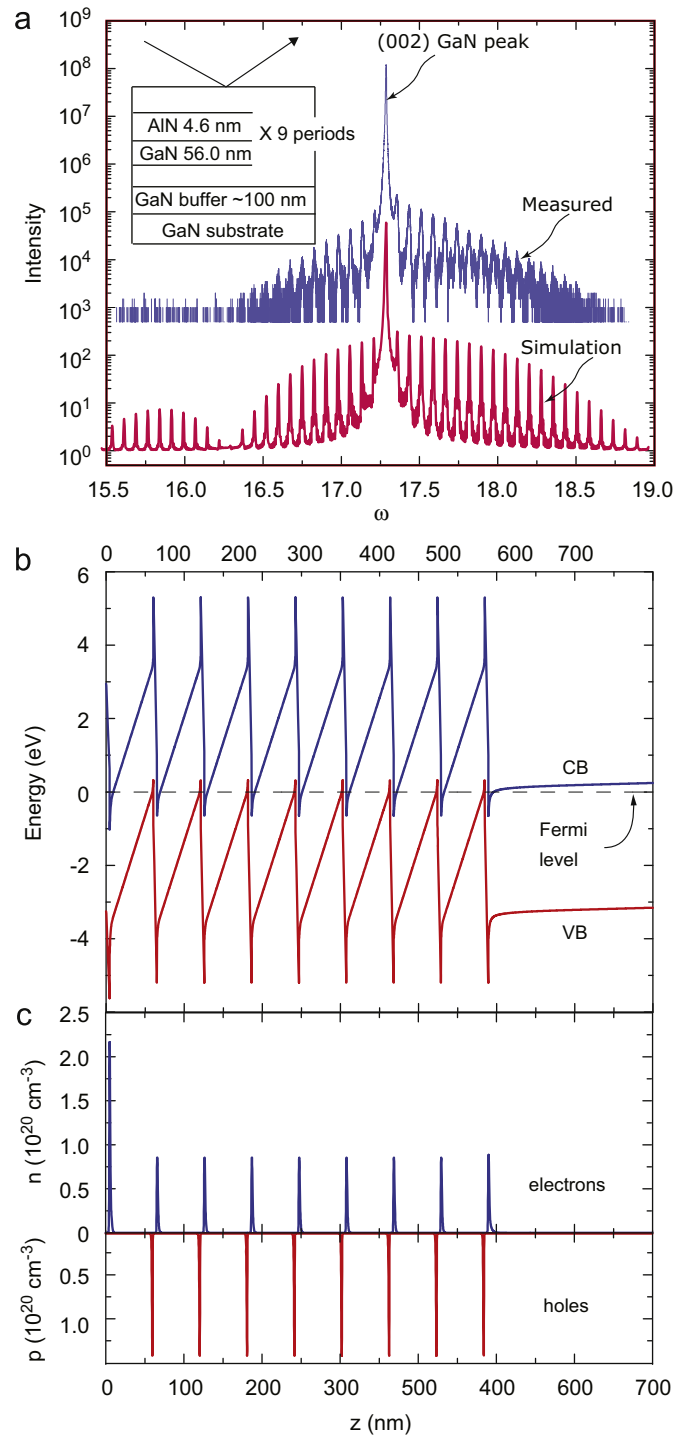


Fig. 6. (a) Measured and calculated (002) GaN X-ray diffraction spectrum for a 9-period AlN/GaN SLs with (b) the SLs band diagram, and (c) electron and hole distribution plotted.

sharp peaks were caused by the interference at different AlN/GaN heterointerfaces. By fitting the measured data to a simulation, the thicknesses of AlN and GaN were extracted to be $a = 4.6 \text{ nm}$ and $b = 56 \text{ nm}$ in each period. In the band diagram, shown in Fig. 6(b), the valence band of GaN reaches the Fermi level at the AlN/GaN interface, indicating both 2DEGs and two dimension hole gases (2DHGs) can be formed in the MQWs. Fig. 6(c) shows the simulated distribution of 2DEGs and 2DHGs along the growth direction. By Hall-effect measurement, the measured sheet charge density is $1.08 \times 10^{14} \text{ cm}^{-2}$ with a

enhanced RT mobility of $1567 \text{ cm}^2/\text{Vs}$. These 2DEGs and 2DHGs are spatially separated, and lateral sheet resistance R_{sh} is as low as $37 \text{ } \Omega/\text{sq}$ at room temperature, whereas vertical resistances are expected to be high due to the AlN barriers. The electron charges at the top AlN/GaN heterointerface are partially from the surface according to charge transfer theory. When holes are generated due to the polarization field at the AlN/GaN heterointerfaces deeper into the structure from the surface, the electrons move to the conduction band, and thus the valence band becomes the source of electrons. With the presented date, it is hard to conclude whether the holes are trapped or mobile. Heikman et al. reported that in periodic $\text{Al}_{0.22}\text{GaN}/\text{GaN}$ structures by introducing heavily doped graded AlGaIn layers, the AlGaIn barrier height can be efficiently lowered [12]. In AlN/GaN MQWs, the conduction band offset ΔE_c between AlN and GaN is much larger compared to that in AlGaIn/GaN MQWs. It may prove difficult to achieve high vertical conductivity due to the high ΔE_c . For device application, further study is needed to enhance the vertical conductivity.

4. Conclusion

The effect of metal flux on 2DEG transport properties in single and multiple MBE-grown AlN/GaN heterojunctions was studied. With the optimized metal fluxes, record-low sheet resistance ($\sim 128 \text{ } \Omega/\text{sq}$) was obtained in an as-grown single AlN/GaN heterostructure. Hall

measurement results showed that multiple 2DEGs existed in the AlN/GaN MQWs. It is possible to have both 2DEGs and 2DHGs existing in the AlN/GaN MQWs. The multiple 2DEG channels provide very low lateral sheet resistance $\sim 37 \text{ } \Omega$ at room temperature.

References

- [1] Y. Cao, K. Wang, A. Orlov, H. Xing, D. Jena, *Appl. Phys. Lett.* 92 (2008) 152112.
- [2] A. Dabiran, A. Wowchak, A. Osinsky, J. Xie, B. Hertog, B. Cui, D. Look, P. Chow, *Appl. Phys. Lett.* 93 (2008) 082111.
- [3] T. Zimmermann, D. Deen, Y. Cao, J. Simon, P. Fay, D. Jena, H. Xing, *IEEE Electron Device Lett.* 29 (2008) 661.
- [4] Y. Cao, T. Zimmermann, H. Xing, D. Jena, *Appl. Phys. Lett.* 96 (2010) 042102.
- [5] Y. Cao, D. Jena, *Appl. Phys. Lett.* 90 (2007) 182112.
- [6] X. Wang, T. Cheng, Z. Ma, G. Hu, H. Xiao, J. Ran, C. Wang, W. Luo, *Solid State Electron.* 51 (2007) 428.
- [7] R. Tülek, A. Ilgaz, S. Gökden, A. Teke, M.K. Öztürk, M. Kasap, S. Özçelik, E. Arslan, E. Özbay, *J. Appl. Phys.* 105 (2009) 013707.
- [8] Y. Kawakami, A. Nakajima, X. Shen, G. Piao, M. Shimizu, H. Okumura, *Appl. Phys. Lett.* 90 (2007) 242112.
- [9] The software is available from the webpage of Prof. Gregory Snider at University of Notre Dame <<http://www.nd.edu/~gsnider>>.
- [10] S. Yamaguichi, Y. Iwamura, Y. Watanabe, M. Kosaki, Y. Yukawa, S. Nitta, S. Kamiyama, H. Amano, I. Akasaki, *Appl. Phys. Lett.* 80 (2002) 802.
- [11] L. Sang, Z. Qin, H. Fang, X. Zhou, Z. Yang, B. Shen, G. Zhang, *Appl. Phys. Lett.* 92 (2008) 192112.
- [12] S. Heikman, S. Keller, D. Green, S. DenBaars, U. Mishra, *J. Appl. Phys.* 94 (2003) 5321.